Interaction of Tl^+ and Cs^+ with the $[Fe_3S_4]$ Cluster of *Pyrococcus furiosus* Ferredoxin: Investigation by Resonance Raman, MCD, EPR, and ENDOR Spectroscopy

Weiguang Fu,[†] Joshua Telser,[§,⊥] Brian M. Hoffman,[§] Eugene T. Smith,[‡] Michael W. W. Adams,[‡] Michael G. Finnegan,[†] Richard C. Conover,[†] and Michael K. Johnson*,[†]

Contribution from the Departments of Chemistry and Biochemistry and Center for Metalloenzyme Studies, University of Georgia, Athens, Georgia 30602, and Department of Chemistry, Northwestern University, Evanston, Illinois 60208

Received February 10, 1994[•]

Abstract: The hyperthermophilic archaeon *Pyrococcus furiosus* contains a novel 4Fe ferredoxin in which one Fe ion lacks cysteinyl coordination. This unique Fe ion can be easily removed to yield protein containing a $[Fe_3S_4]^0$ cluster. Under reducing conditions, this cluster can bind exogenous metal dications, M^{2+} (e.g., Ni^{2+} and Zn^{2+}), to yield $[MFe_3S_4]^+$ clusters. In this work, we have investigated the affinity of the $[Fe_3S_4]^{0,+}$ cluster in *P. furiosus* ferredoxin for the monocations Cs^+ and Tl^+ in the absence of reducing agents. Both of these metal ions are large and polarizable, but they differ greatly in their propensity for ionic versus covalent interactions. The structural, electronic, and magnetic properties of the $[Fe_3S_4]^{0,+}$ cluster in *P. furiosus* ferredoxin in the presence of excess Cs^+ and Tl^+ were studied by EPR, magnetic circular dichroism, resonance Raman, and electron–nuclear double resonance spectroscopy. Magnetic circular dichroism and resonance Raman studies indicate that Tl^+ but not Cs^+ is incorporated into the reduced $[Fe_3S_4]^0$ cluster with retention of the $S = 2$ ($D < 0$) ground state to yield a $[TlFe_3S_4]^+$ cluster. EPR studies provide evidence for Tl^+ incorporation into the oxidized $S = {}^1/_2$ $[Fe_3S_4]^+$ cluster as well. The native protein exhibits a broad EPR signal as a result of the distribution of g-values from multiple cluster conformations. In the presence of excess Tl^+, a much narrower axial EPR signal is observed, indicating a single cluster conformation. Furthermore, $^{203,205}Tl$ hyperfine coupling was observed at both 9 and 35 GHz. The large coupling constant, $A^{Tl} \approx 370$ MHz (13 mT), indicates a covalent interaction associated with the formation of $[TlFe_3S_4]^{2+}$. In contrast, the presence of excess Cs^+ does not change the EPR spectrum, nor is ^{133}Cs hyperfine coupling observed, indicating a failure to incorporate this ion. However, ^{133}Cs electron–nuclear double resonance signals were observed with hyperfine and quadrupole couplings of $A^{Cs} \approx 1.2$ MHz, $P_z \approx 0.7$ MHz. This, in conjunction with resonance Raman data, suggests that a Cs^+ ion binds to a specific residue near the oxidized cluster. This is the first report of ^{133}Cs ENDOR in a biological system and suggests that this readily available nucleus could provide a valuable probe for Na^+ or K^+ binding in paramagnetic biomolecules.

Introduction

Several iron–sulfur proteins are now known in which the Fe–S cluster functions as the active site of chemical catalysis, as opposed to the more conventional electron transport role associated with these clusters in ferredoxins (Fds).[1] Examples include aconitase,[2] several (de)hydratases,[3] sulfite reductase,[4] nitrogenase,[5] hydrogenase,[6] and CO dehydrogenase.[7] For example where X-ray crystal structures are available, the catalytically active Fe–S clusters have been found to be based on a cubane-type $[Fe_4S_4]$ structural unit that lacks cysteinyl ligation at a specific Fe site and/or that has replacement of a specific Fe with another transition metal. Aconitase is the best characterized example of the former. Spectroscopic (EPR, ENDOR, and Mössbauer) and X-ray crystallographic studies have shown the substrate to be bound to specific Fe atom that has been made coordinatively unsaturated by the absence of the cysteinyl ligand.[2] Nitrogenase provides an example of the latter type of active site cluster. This cluster can be viewed as a fusion of cubane-type $[Fe_4S_3]$ and $[MoFe_3S_4]$ fragments bridged by three μ_2-S^{2-} bridges.[5] However, the X-ray crystallographic studies indicate that the Mo is coordinatively saturated and may not be the site of N_2 activation.[5] In sulfite reductase, the active site consists of a siroheme linked in an as yet undetermined way to a $[Fe_4S_4]$ cluster.[4] The structures of the homometallic H_2-activating Fe–S cluster in Fe-only hydrogenases and of the heterometallic Ni–Fe–S clusters at the active sites of CO dehydrogenases and acetyl-CoA synthases have yet to be determined.

This potential for heterometallic cubane-type clusters to participate in enzymatic catalysis has stimulated interest in their reactivity and properties. Holm and co-workers have synthesized and characterized a wide range of crystallographically-defined

[†] Department of Chemistry and Center for Metalloenzyme Studies, University of Georgia.
[‡] Department of Biochemistry and Center for Metalloenzyme Studies, University of Georgia.
[§] Department of Chemistry, Northwestern University.
[⊥] Permanent address: Department of Chemistry, Roosevelt University, 430 S. Michigan Ave., Chicago, IL 60605.
* Address correspondence to this author at Department of Chemistry, University of Georgia, Athens, GA 30602. Tel: 706-542-9378. FAX: 706-542-9454. e-mail: johnson@sunchem.chem.uga.edu.
• Abstract published in *Advance ACS Abstracts*, June 1, 1994.

(1) Abbreviations used: Fd, ferredoxin; MCD, magnetic circular dichroism, RR, resonance Raman; ENDOR, electron–nuclear double resonance; ESEEM, electron spin echo envelope modulation; rf, radio frequency, S^b, bridging or inorganic sulfur; S^t, terminal or cysteinyl sulfur; sh, shoulder.

(2) (a) Beinert, H.; Kennedy, M. C. *Eur. J. Biochem.* **1989**, *186*, 5–15. (b) Werst, M. M.; Kennedy, M. C.; Beinert, H.; Hoffman, B. M. *Biochemistry* **1990**, *29*, 10526–10532. (c) Kennedy, M. C.; Stout, C. D. *Adv. Inorg. Chem.* **1992**, *38*, 323–339. (d) Lauble, H.; Kennedy, M. C.; Beinert, H.; Stout, C. D. *Biochemistry* **1992**, *31*, 2735–2748.

(3) Flint, D.; H.; Emptage, M. H.; Finnegan, M. G.; Fu, W.; Johnson, M. K. *J. Biol. Chem.* **1993**, *268*, 14732–14742 and references therein.

(4) (a) Christner, J. A.; Münck, E.; Janick, P. A.; Siegel, L. M. *J. Biol. Chem.* **1981**, *256*, 2098–2101. (b) McRee, D. E.; Richardson, D. C.; Richardson, J. S.; Siegel, L. M. *J. Biol. Chem.* **1986**, *261*, 10277–10281.

(5) (a) Kim, J.; Rees, D. C. *Science* **1992**, *257*, 1677–1682. (b) Chan, M. K.; Kim, J.; Rees, D. C. *Science* **1993**, *260*, 792–794.

(6) Adams, M. W. W. *Biochim. Biophys. Acta* **1990**, *1020*, 115–145.

(7) (a) Stephens, P. J.; McKenna, M-C.; Ensign, S. A.; Bonam, D.; Ludden, P. A. *J. Biol. Chem.* **1989**, *264*, 16347–16350. (b) Fan, C.; Gorst, C. M.; Ragsdale, S. W.; Hoffman, B. M. *Biochemistry* **1991**, *30*, 431–435 and references therein.

0002-7863/94/1516-5722$04.50/0

clusters containing $[MFe_3S_4]$ cores (M = Ni, Co, Mo, W, V, Re, Nb).[8] The ability of $[Fe_3S_4]^0$ clusters in simple Fds to take up exogenous divalent and trivalent metal ions under reducing conditions to yield heterometallic $[MFe_3S_4]^{2+/+}$ clusters (M = Co^{2+}, Zn^{2+}, Ni^{2+}, Cd^{2+}, Ga^{3+}) has been demonstrated spectroscopically by Moura and co-workers using *Desulfovibrio gigas* Fd II.[9] Similar studies have been reported using the 3Fe/4Fe Fd from *Pyrococcus furiosus* (M = Ni^{2+}, Zn^{2+}, Co^{2+}, Mn^{2+})[10] and a 7Fe/8Fe Fd from *Desulfovibrio africanus* (M = Zn^{2+} and Cd^{2+}).[11] While heterometallic $[MFe_3S_4]$ clusters have yet to be established as the active site of any metalloenzyme, this body of work has greatly enhanced our understanding of the magnetic, redox, and ligand-binding properties of both heterometallic and homometallic cubane clusters.

P. furiosus Fd is a small monomeric protein (M_r = 7500) containing a single $[Fe_4S_4]$ cluster.[12] It is remarkable both for its extreme thermal stability (stable at 95 °C for at least 12 h) and because it provided the only example of a 4Fe Fd that has non-cysteinyl ligation of one Fe atom, as evidenced by the replacement of a ligating residue by an aspartic acid residue in the amino acid sequence.[12,13] Non-cysteinyl ligation of one Fe is manifest in the novel spectroscopic properties of the $[Fe_4S_4]^{2+/+}$ cluster,[12] the ease of quantitative removal of this Fe atom under oxidizing conditions to yield a conventional $[Fe_3S_4]^{+/0}$ cluster,[12,13] and the ability of the cluster to bind exogenous ligands such as CN^-.[14] The properties of *P. furiosus* Fd make it an ideal system for forming and investigating the physical and ligand-binding properties of $[MFe_3S_4]$ clusters in a biological environment.[10]

Thus, far, there has been only one report of exogenous metal binding to an oxidized $[Fe_3S_4]^+$ cluster. Butt *et al.* provided electrochemical evidence for binding the monocation Tl^+ to the $[Fe_3S_4]^{+,0}$ cluster in the 7Fe Fd from *D. africanus*.[15] However, spectroscopic evidence in the form of $^{203,205}Tl$ hyperfine splitting of the EPR signal or structural/electronic perturbations revealed by RR/MCD studies were not forthcoming. Here we compare the affinity of the $[Fe_3S_4]^{+,0}$ clusters in *P. furiosus* Fd for two large, polarizable, monovalent cations, Tl^+ and Cs^+, and explore the structural, electronic, and magnetic properties of the resulting heterometallic clusters using the combination of EPR, magnetic circular dichroism (MCD), resonance Raman (RR), and electron–nuclear double resonance (ENDOR) spectroscopy. The ionic radii of these cations, 167 and 150 pm for Cs^+ and Tl^+, respectively, are among the largest known.[16] However, they exhibit very different behaviors regarding sulfide binding in aqueous solution (e.g., Cs_2S is very water soluble, while for Tl_2S, $K_{SP} = 1 \times 10^{-22}$) as a result of predominantly ionic (Cs^+) versus covalent (Tl^+) interactions. This difference is manifest in the interaction of these monocations with the $[Fe_3S_4]^{0,+}$ cluster in *P. furiosus* Fd. The results presented herein demonstrate that both the oxidized and reduced $[Fe_3S_4]$ clusters incorporate Tl^+ to form $[TlFe_3S_4]^{+,2+}$, but neither form incorporates Cs^+ into the cluster. However, Cs^+ does appear to bind to a residue in close proximity to the $[Fe_3S_4]^+$ cluster in the oxidized protein.

Experimental Methods and Theory

Sample Preparation. *P. furiosus* was grown and the ferredoxin purified anaerobically in the presence of 2 mM sodium dithionite as previously described.[17] The 3Fe form was prepared by incubating the air-oxidized Fd with a 5-fold excess of potassium ferricyanide and a 10-fold excess of EDTA at room temperature for 30 min, followed by gel filtration (Sephadex G-25) to remove excess reagents. Sample concentrations for the 3Fe Fd were based on protein determinations[18] using apoprotein prepared by precipitation with trichloroacetic acid and/or EPR spin quantitations. These methods agreed to within 10%. Samples of the oxidized or dithionite-reduced 3Fe Fd in 50 mM Tris-HCl buffer, pH 7.8, were treated with a 1–1000-fold excess of CsCl or $Tl(OOCCH_3)$ and incubated at room temperature for 30 min prior to freezing for spectroscopic measurements.

Spectroscopic Instrumentation. Variable-temperature and variable-field MCD measurements were recorded on samples containing 50% (v/v) ethylene glycol using a Jasco J-500C (180–1000 nm) or J-730 (700–2000 nm) spectropolarimeter mated to an Oxford Instruments SM3 split coil superconducting magnet. The experimental protocols for measuring MCD spectra of oxygen-sensitive samples over the temperature range 1.5–300 K with magnetic fields up to 5 T have been described elsewhere.[19] Raman spectra were recorded with an Instruments SA U1000 spectrometer fitted with a cooled RCA 31034 photomultiplier tube, using lines from a Coherent Innova 100 10-W Ar^+ or 200-K2 Kr^+ laser. Scattering was collected at 90° from the surface of a frozen 10-μL droplet of protein on the cold finger of an Air-Products Displex Model CSA-202E closed-cycle refrigerator. Further details of the Raman spectrometer and the protocols used for obtaining low-temperature spectra of frozen anaerobic protein solutions are given elsewhere.[20] X-band (~9.5 GHz) EPR spectra were recorded on a Bruker ESP-300E EPR spectrometer equipped with an Oxford Instruments ESR-9 flow cryostat. Spin quantitations were carried out under nonsaturating conditions using 1 mM CuEDTA as the standard. Q-band (35 GHz) EPR and ENDOR spectra were recorded on a modified Varian E-109 spectrometer equipped with a liquid helium immersion dewar, as described elsewhere.[21] All Q-band spectra were recorded at 2 K and in dispersion mode, under "rapid-passage" conditions.[22]

ENDOR Theory. The single-crystal ENDOR spectrum of nucleus J, of spin $I = {}^1/_2$ (e.g., ^1H, $^{203,205}Tl$), consists of two lines whose frequencies are given by eq 1:

$$\nu_\pm = |\nu_J \pm A^J/2| \tag{1}$$

where A^J is the orientation-dependent nuclear hyperfine coupling constant and ν_J is the nuclear Larmor frequency. For a quadrupolar nucleus J, with $I \geq 1$ (e.g., ^{133}Cs, $I = {}^7/_2$), the ENDOR pattern is further split into $2I$ lines with the frequencies given to first order by eq 2.[23]

$$\nu_\pm(m) = |\nu_J \pm A^J/2 + 3P^J(2m-1)/2| \tag{2}$$

where $-I + 1 \leq m \leq I$ and this splitting is governed by P^J, the orientation-dependent quadrupole coupling constant. However, if the hyperfine and quadrupole terms are comparable in energy, then a complex, non-first-order pattern can result.[23] Analysis of ^{133}Cs ENDOR also was performed using a FORTRAN program that diagonalizes the complete spin Hamiltonian matrix for $S = {}^1/_2$, $0 < I \leq {}^7/_2$ systems[23] and generates the ENDOR transition frequencies and nuclear magnetic dipole transition

(8) Holm, R. H. *Adv. Inorg. Chem.* **1992**, *38*, 1–71.
(9) (a) Moura, I.; Moura, J. J. G.; Münck, E.; Papaefthymiou, V.; LeGall, J. *J. Am. Chem. Soc.* **1986**, *108*, 349–351. (b) Surerus, K. K.; Münck, E.; Moura, I.; Moura, J. J. G.; LeGall, J. *J. Am. Chem. Soc.* **1987**, *109*, 3805–3807. (c) Surerus, K. K., Ph.D. Thesis, University of Minnesota, Minneapolis, MN, 1989.
(10) (a) Conover, R. C.; Park, J.-B.; Adams, M. W. W.; Johnson, M. K. *J. Am. Chem. Soc.* **1990**, *112*, 4562–4564. (b) Srivastava, K. K. P.; Surerus, K. K.; Conover, R. C.; Johnson, M. K.; Park, J.-B.; Adams, M. W. W.; Münck, E. *Inorg. Chem.* **1993**, *32*, 927–936. (c) Conover, R. C., Ph.D. Thesis, University of Georgia Athens, GA, 1993.
(11) Butt, J. N.; Armstrong, F. A.; Breton, J.; George, S. J.; Thomson, A. J.; Hatchikian, E. C. *J. Am. Chem. Soc.* **1991**, *113*, 6663–6670.
(12) Conover, R. C.; Kowal, A. T.; Fu, W.; Park, J.-B.; Aono, S.; Adams, M. W. W.; Johnson, M. K. *J. Biol. Chem.* **1990**, *265*, 8533–8541.
(13) Busse, S. C.; La Mar, G. N.; Yu, L.-P.; Howard, J. B.; Smith, E. T.; Zhou, Z. H.; Adams, M. W. W. *Biochemistry* **1992**, *31*, 11952–11962.
(14) Conover, R. C.; Park, J.-B.; Adams, M. W. W.; Johnson, M. K. *J. Am. Chem. Soc.* **1991**, *113*, 2799–2800.
(15) Butt, J. N.; Sucheta, A.; Armstrong, F. A.; Breton, J.; Thomson, A. J.; Hatchikian, E. C.; *J. Am. Chem. Soc.* **1991**, *113*, 8948–8950.
(16) Shannon, R. D. *Acta Crystallogr.* **1976**, *A32*, 751–767.
(17) Aono, S.; Bryant, F. O.; Adams, M. W. W. *J. Bacteriol.* **1989**, *171*, 3433–3439.
(18) Lowery, O. H.; Rosebrough, N. J.; Farr, A. L.; Randall, R. J. *J. Biol. Chem.* **1951**, *193*, 265–275.
(19) Johnson, M. K. In *Metal Clusters in Proteins*; Que, L., Jr., Ed.; ACS Symposium Series 372; American Chemical Society: Washington, DC, 1988; pp 326–342.
(20) Hamilton, C. L.; Scott, R. A.; Johnson, M. K. *J. Biol. Chem.* **1989**, *264*, 11605–11613.
(21) Gurbiel, R. J.; Batie, C. J.; Sivaraja, M.; True, A. E.; Fee, J. A.; Hoffman, B. M.; Ballou, D. P. *Biochemistry* **1989**, *28*, 4861–4871.
(22) Kevan, L.; Kispert, L. D. *Electron Spin Double Resonance Spectroscopy*; Wiley: New York, 1976.
(23) Abragam, A.; Bleaney, B. *Electron Paramagnetic Resonance of Transition Ions*; Clarendon: Oxford, U.K., 1970; pp 166–167, 225–228.
(24) Bennett, D. E.; Johnson, M. K. *Biochim. Biophys. Acta* **1987**, *911*, 71–80.

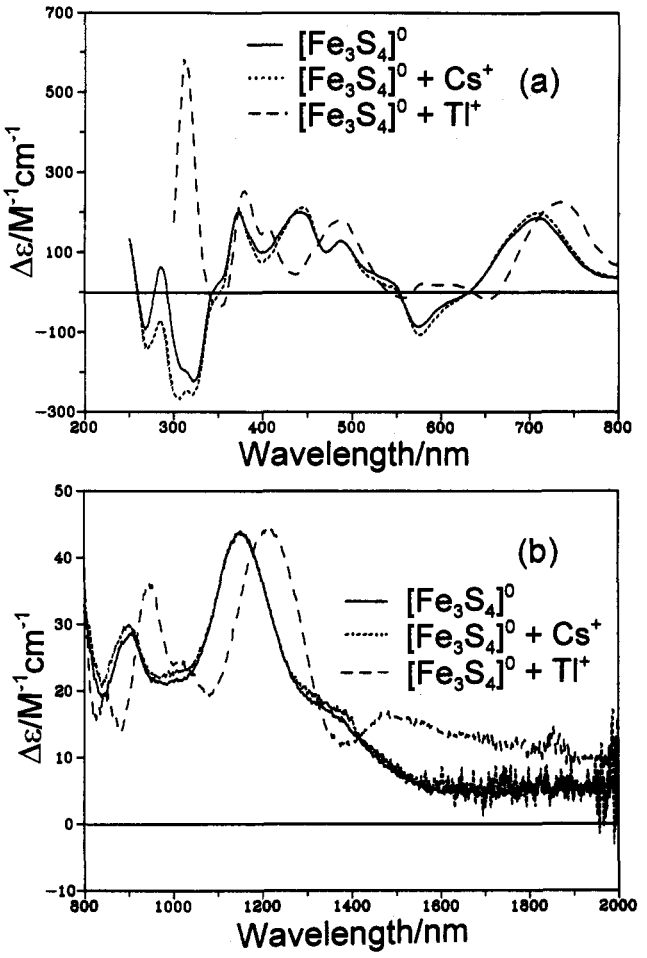

Figure 1. Low-temperature MCD spectra of the dithionite-reduced $[Fe_3S_4]^0$ cluster in *P. furiosus* Fd in the presence of excess Cs^+ and Tl^+. Solid line: as prepared. Dashed line: plus 30-fold molar excess of Tl-($OOCCH_3$). Dotted line: plus 30-fold molar excess of CsCl. All the samples were approximately 0.29 mM in Fd in 50 mM Tris-HCl buffer, pH 7.8, with 2 mM dithionite and 55% (v/v) ethylene glycol. MCD spectra were recorded with a magnetic field of 4.5 T and temperature of 4.2 K in (a) UV–visible region and (b) near-IR region.

probabilities from the eigenstates and eigenvectors, respectively. A Gaussian or Lorentzian line shape is then convoluted to the "stick pattern" obtained in this manner to similate an experimental spectrum.

Results and Discussion

Addition of Excess Cs^+ and Tl^+ to the Reduced $[Fe_3S_4]^0$ Cluster. Variable-temperature and variable-field MCD measurements provide sensitive monitors of the ground- and excited-state properties of paramagnetic Fe–S clusters and hence useful criteria for assessing exogenous metal binding to $S = 2$ $[Fe_3S_4]^0$ clusters.[19] The effect of a 30-fold excess of Cs^+ and Tl^+ on the low-temperature UV/visible/near-IR MCD spectra of the reduced 3Fe form of *P. furiosus* Fd are shown in Figure 1. In each case, the spectra are strongly temperature dependent, with all bands increasing in intensity with decreasing temperature. No significant changes were observed with Cs^+, even with excesses up to 100-fold, and the MCD data clearly do not support the formation of a well-defined $[CsFe_3S_4]^+$ cluster in which the Cs^+ is attached by a covalent interaction. In contrast, a 10-fold excess of Tl^+ effected dramatic changes in the low-temperature MCD spectrum, and increasing the excess to 30-fold resulted in no further changes. The visible/near-IR bands that arise from S → Fe(III) charge-transfer transitions are shifted to lower energy by between 600 and 1600 cm^{-1} for the sample treated with Tl^+, but their signs and relative intensities are not significantly perturbed, suggesting that the $[Fe_3S_4]^0$ fragment is left intact. The MCD

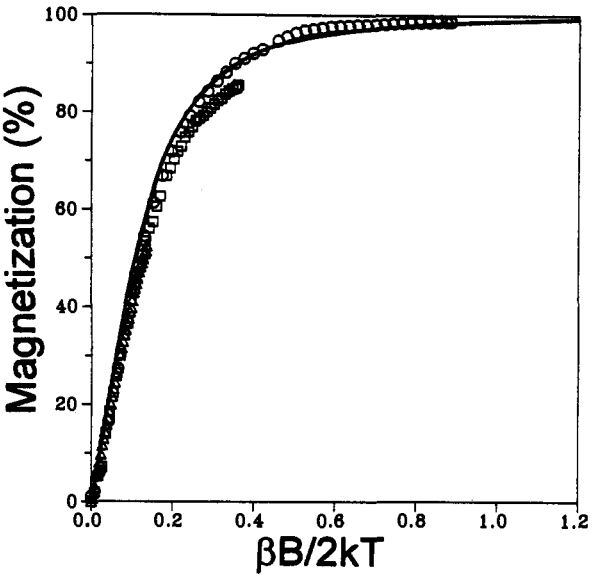

Figure 2. MCD magnetization plot for the dithionite-reduced $[TlFe_3S_4]^+$ cluster in *P. furiosus* Fd. Samples are as described in Figure 1. MCD magnetization data collected at 735 nm. Temperatures: ○, 1.7 K; □, 4.2 K; △, 11.1 K. Magnetic fields were between 0 and 4.5 T. The solid line is the theoretical magnetization curve for an *xy*-polarized transition originating from an isolated doublet with effective *g*-values, $g_\parallel = 8.00$ and $g_\perp = 0.00$.[24]

is therefore consistent with the formation of a $[TlFe_3S_4]^+$ cluster, since covalent binding of Tl^+ to the three μ_2-S atoms of the $[Fe_3S_4]^0$ fragment would be expected to perturb the energy of S → Fe(III) charge-transfer transitions by changing the energy of the predominantly S-based molecular orbitals. The intense positive MCD band at 310 nm that appears on Tl binding is attributed to a charge-transfer or $d^{10} \rightarrow$ s or p transition localized on Tl(I).

MCD magnetization and X-band EPR studies indicate that Tl^+ binding has little effect on the ground-state properties of the $[Fe_3S_4]^0$ fragment, see Figure 2. As is the case for the $[Fe_3S_4]^0$ cluster,[14] the magnetization data at the lowest temperature are well fit by theoretical data constructed for an *xy*-polarized transition from the lowest $M_S = \pm 2$ doublet of a $S = 2$ ground state with $D < 0$ (i.e., $g_\parallel = 8.0$ and $g_\perp = 0.0$). In accord with this, the $[TlFe_3S_4]^+$ cluster in *P. furiosus* Fd exhibits a broad EPR signal centered aroung $g \approx 10$ very similar to that observed for the native $[Fe_3S_4]^0$ cluster.[14] By analogy with other $[Fe_3S_4]$-containing ferredoxins,[25] this resonance is assigned to the formally forbidden transition within the $M_S = \pm 2$ doublet of the $S = 2$ ground state.

Resonance Raman provides a direct method for investigating structural perturbations at biological Fe–S clusters via changes in Fe–S stretching frequencies.[26] Published RR studies of $[Fe_3S_4]^0$ clusters have been limited to room-temperature spectra for reduced *D. gigas* Fd II.[27] High-quality low-temperature RR spectra of the reduced $[Fe_3S_4]^0$ cluster in *P. furiosis* Fd have recently been obtained with laser excitation in the range 457.9–514.5 nm and tentatively assigned based on $^{34}S^b$-isotope shifts[28] under effective C_s symmetry.[29] The spectrum with 457.9-nm excitation is shown in Figure 3a. The bands at 319, 334, and 349 cm^{-1} are assigned primarily to Fe–S^t stretching (≤3-cm^{-1} $^{34}S^b$-downshifts), whereas

(25) (a) Hagen, W. R.; Dunham, W. R.; Johnson, M. K.; Fee, J. A. *Biochim. Biophys. Acta* **1985**, *828*, 369–374. (b) Papaefthymiou, V.; Girerd, J.-J.; Moura, I.; Moura, J. J. G.; Münck, E. *J. Am. Chem. Soc.* **1987**, *109*, 4703–4710.

(26) Spiro, T. G.; Czernuszewicz, R. S.; Han, S. In *Resonance Raman Spectra of Heme and Metalloproteins*; Spiro, T. G., Ed.; Biological Applications of Raman Spectroscopy 3; Wiley: New York, 1988; pp 523–553.

(27) Johnson, M. K.; Hare, J. W.; Spiro, T. G.; Moura, J. J. G.; Xavier, A. V.; LeGall, J. *J. Biol. Chem.* **1981**, *256*, 9806–9808.

(28) (a) Fu, W., M.S. Thesis, University of Georgia Athens, GA, 1990. (b) Fu, W.; Park, J.-B.; Adams, M. W. W.; Johnson, M. K., manuscript in preparation.

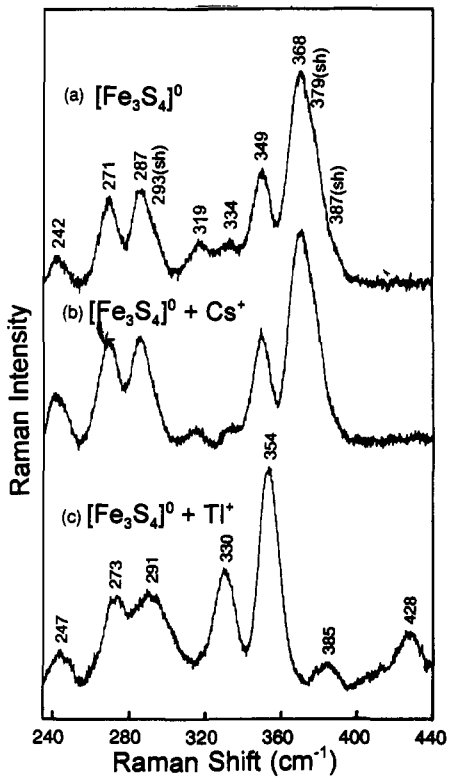

Figure 3. Low-temperature resonance Raman spectra of the dithionite-reduced $[Fe_3S_4]^0$ cluster in *P. furiosus* Fd in the presence of excess Cs^+ and Tl^+. (a) As prepared; (b) with 30-fold molar excess of CsCl; and (c) with 30-fold molar excess of $Tl(OOCCH_3)$. All the samples were approximately 2 mM in Fd in 50 mM Tris-HCl, pH = 7.8, and 2 mM in sodium dithionite. The spectra were obtained at 17 K using 457.9-nm laser excitation and are the sum of 36 scans. Each scan involved photon counting for 1 s at 0.2-cm^{-1} increments with 6-cm^{-1} spectral resolution. Bands arising from the frozen dithionite/buffer solution have been subtracted.

the bands at 242, 271, 287, 293(sh), 368, 379(sh), and 387(sh) cm^{-1} predominantly involve Fe–S^b stretching (≥5-cm^{-1} $^{34}S^b$-downshifts). RR studies reveal that excess Tl^+ but not Cs^+ effects structural perturbation of the $[Fe_3S_4]^0$ cluster, see Figure 3. While detailed vibrational assignments will require $^{34}S^b$-isotope shift data and normal mode calculations, the pronounced changes in the RR spectrum clearly support complete conversion to a $[TlFe_3S_4]^+$ cluster on addition of a 30-fold excess of Tl^+ to the $[Fe_3S_4]^0$ cluster. The absence of any significant shift in the RR spectrum for samples treated with up to a 50-fold molar excess of Cs^+ provides further evidence against the formation of a $[CsFe_3S_4]^+$ cluster.

The MCD and RR data presented above provide spectroscopic support for the results of Butt *et al.*,[15] who reported high-affinity binding of Tl^+ to the $[Fe_3S_4]^0$ cluster in *D. africanus* Fd III based on the electrochemical studies. Moreover, the spectroscopic changes are clearly consistent with binding to the tri-μ_2-sulfido face of the $[Fe_3S_4]^0$ cluster. This is further supported by the observation that Tl^+ excesses up to 1000-fold do not perturb the electronic, magnetic, or structural properties of the $[Fe_4S_4]^{2+/+}$ cluster in *P. furiosus* Fd, as evidenced by EPR, MCD, and RR studies and by the observation that Tl^+ binding is completely reversible. Tl^+ is readily lost under oxidizing conditions in the absence of excess Tl^+ to yield the $[Fe_3S_4]^+$ cluster, which avidly takes up Tl^+ again, under reducing conditions.

Addition of Excess Cs^+ and Tl^+ to the Oxidized $[Fe_3S_4]^+$ Cluster. Evidence for interaction of Tl^+ and Cs^+ with the oxidized $[Fe_3S_4]^+$ cluster comes primarily from EPR and ENDOR studies. The EPR spectrum of oxidized 3Fe *P. furiosus* Fd consists of a fast-relaxing signal that is only observable at $T < 30$ K.[12] It has a well-defined g-value only at the low-field ($g = 2.03$); extending to higher field, there is only a broad, featureless signal. Similar EPR signals, although varying in signal breadth and relaxation properties, have been observed for all known $[Fe_3S_4]^+$ clusters.[30] Guigliarelli *et al.* have provided a theoretical basis for this anomalous EPR behavior,[31] and recent experimental studies support this explanation.[32] It arises because individual protein molecules have slightly different cluster conformations. These varying microenvironments lead to a distribution of zero-field splitting parameters for the individual cluster Fe^{3+} ions (D_i) and of antiferromagnetic coupling parameters between cluster Fe^{3+} ions (J_{ij}). This distribution in D_i and J_{ij} leads to a distribution of g-values and a broad, fast-relaxing EPR spectrum. For $[Fe_3S_4]^+$ in *P. furiosus* Fd, the spectrum is particularly broad, perhaps indicating a relatively plastic cluster environment, compared to other proteins.

Butt *et al.* reported that the oxidized $[Fe_3S_4]^+$ cluster in *D. africanus* Fd III had weak affinity for Tl^+ based on electrochemical studies and that the isotropic $g = 2.01$ EPR associated with this cluster (i.e., relatively narrow g-distribution) was converted at X-band to a "rhombic" spectrum with $g = 2.042$, 1.993, and 1.954 in the presence of a 760-fold excess of Tl^+.[15] Thus, these new EPR features were attributed to a cluster–Tl^+ interaction that led to a changed electronic configuration for the cluster (different g-values) but no concomitant hyperfine coupling from the Tl^+ nucleus. This result was surprising, given the large nuclear moments of the two magnetically almost identical thallium nuclei (^{203}Tl, $I = {}^1/_2$, $g_N = 3.2445$, 29.5% natural abundance; ^{205}Tl, $I = {}^1/_2$, $g_N = 3.2754$, 70.5% natural abundance). In fact, $^{203,205}Tl$ has the fourth largest magnitude g_N for stable nuclei (after ^1H, ^{19}F, and ^3He).[33] As a result, hyperfine coupling constants for thallium-centered radicals are quite large. Irradiation by γ-rays of Tl^+ and Tl^{3+} nitrate and perchlorate salts produced Tl^{2+}, which had a hyperfine coupling constant of ~4 T.[34] Radicals derived from the counterions were also produced and gave widely varying $^{203,205}Tl$ hyperfine coupling constants, with 10–30 mT being typical. Ion pairs between organothallium(III) complexes (R_2Tl^+) and semiquinone radicals gave $^{203,205}Tl$ coupling constants ranging from 1 to 10 mT.[35] Additionally, there are relevant biological studies. Pyruvate kinase, in which VO^{2+} and Tl^+ were substituted for physiological Mg^{2+} and K^+, respectively, gave $^{203,205}Tl$ superhyperfine coupling of ~3 mT.[36] This substitution was also employed in a study of *S*-adenosylmethionine synthetase and yielded $^{203,205}Tl$ superhyperfine coupling of 2.3 mT (67 MHz).[37]

As shown in Figure 4, addition of 1000-fold stoichiometric excess $Tl(OOCCH_3)$ to the oxidized 3Fe form of *P. furiosus* Fd in fact gives a spectrum that can be interpreted as exhibiting a large $^{203,205}Tl$ hyperfine coupling, $A(Tl) \approx 13$ mT. Even with this large excess, Tl^+ binding to the $[Fe_3S_4]^+$ cluster is not quantitative, and resonances from both the unbound and Tl-bound clusters are distinguishable as a result of their markedly

(29) Effective C_s symmetry for the $Fe_3S_4{}^bS_3{}^t$ core comes from Mössbauer studies which indicate that the $S = 2$ ground state arises from coupling between a valence-delocalized Fe^{3+}/Fe^{2+} pair ($S = {}^9/_2$) and a trapped-valence Fe^{3+} site ($S = {}^5/_2$).[10b]

(30) (a) Beinert, H.; Thomson, A. J. *Arch. Biochem. Biophys.* **1983**, *222*, 333–361. (b) Knaff, D. B.; Hirasawa, M.; Ameyibor, E.; Fu, W.; Johnson, M. K. *J. Biol. Chem.* **1991**, *266*, 15080–15084.
(31) Guigliarelli, B.; More, C.; Bertrand, P.; Gayda, J. P. *J. Chem. Phys.* **1986**, *85*, 2774–2778.
(32) (a) Fan, C. L.; Houseman, A. L. P.; Doan, P.; Hoffman, B. M. *J. Phys. Chem.* **1993**, *97*, 3017–3021. (b) Doan, P. E.; Fan, C.; Hoffman, B. M. *J. Am. Chem. Soc.* **1994**, *116*, 1033–1041.
(33) Fuller, G. H. *J. Phys. Chem. Ref. Data* **1976**, *5*, 835.
(34) Symons, M. C. R.; Zimmerman, D. N. *J. Chem. Soc., Dalton Trans.* **1976**, 180–184.
(35) (a) Stegmann, H. B.; Ulmschneider, K. B.; Hieke, K.; Scheffler, K. *J. Organomet. Chem.* **1976**, *118*, 259–287. (b) Stegmann, H. B.; Ulmschneider, K. B.; Schuler, P.; Jülich, T.; Scheffler, K. *Z. Naturforsch.* **1984**, *39b*, 1416–1424.
(36) Lord, K. A.; Reed, G. H. *Inorg. Chem.* **1987**, *26*, 1464–1466.
(37) Markham, G. D.; Leyh, T. S. *J. Am. Chem. Soc.* **1987**, *109*, 599–600.

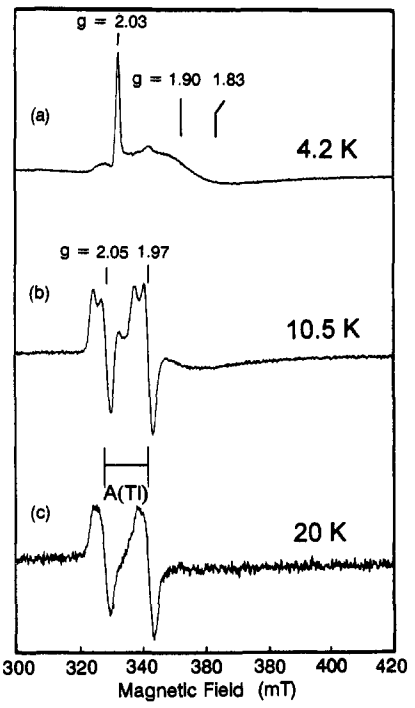

Figure 4. X-band EPR spectra of the oxidized $[Fe_3S_4]^+$ cluster in *P. furiosus* Fd in the presence of a 1000-fold molar excess of $Tl(OOCCH_3)$. The sample was 0.29 mM in Fd in 50 mM Tris-HCl buffer, pH 7.8, with 55% (v/v) ethylene glycol. Experimental conditions: temperature, (a) 4.2 K, (b) 10.5 K, and (c) 20 K; microwave frequency, 9.43 GHz; modulation amplitude, 0.63 mT; microwave power, 1 mW.

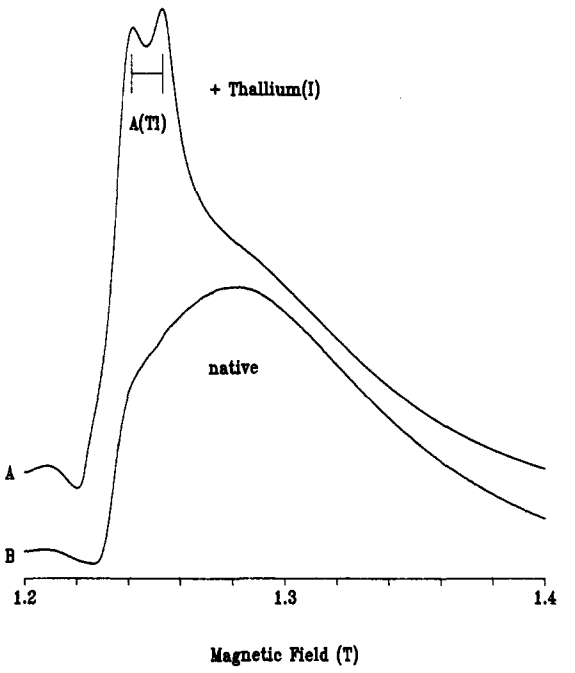

Figure 5. Q-band EPR spectra of the oxidized $[Fe_3S_4]^+$ cluster in *P. furiosus* Fd in the presence (A) and absence (B) of a 1000-fold molar excess of $Tl(OOCCH_3)$. Samples are as described in Figure 4. Experimental conditions: temperature, 2 K; time constant, 32 ms; microwave frequency, 35.08 GHz (Tl^+-treated) and 35.07 GHz (native); microwave power, 0.05 mW; 100-kHz magnetic field modulation amplitude, 0.1 mT. The relative intensities of the native and Tl^+-treated samples are arbitrary; no attempt at normalization was made. The $^{203,205}Tl$ hyperfine-split doublet ($A(Tl) \sim 13$ mT) is indicated.

different relaxation properties. This is illustrated in Figure 4, which shows X-band EPR spectra at 4.2, 10.5, and 20.1 K. At 4.2 K, the spectrum is dominated by the fast-relaxing "$g = 2.03$ resonance" of the native $[Fe_3S_4]^+$. At 10.5 K, the $[Fe_3S_4]^+$ signal becomes significantly broadened into the base line, and two well-resolved axial-shaped features centered at $g = 2.05$ and 1.97 are apparent. At 20 K, the native cluster is no longer observable, and there is a well-defined doublet signal, although the axial line shape is no longer resolved. The doublet splitting is 13.3 mT and is attributed to an isotropic $^{203,205}Tl$ hyperfine interaction. To determine the extent of binding, spin quantitations were carried out at 20 K over a narrow field range and compared with values obtained at 4.2 K over a much wider field range under conditions such that neither signal was saturated. For samples containing 55% (v/v) ethylene glycol and a 1000-fold excess of Tl^+, ~20% of the protein molecules contained a Tl^+-bound cluster. Without ethylene glycol, the Tl^+-bound fraction for equivalent samples was ~10%.

Confirmation that the well-resolved doublet X-band EPR signal of the Tl^+-treated sample arises from $^{203,205}Tl$ hyperfine interaction, as opposed to a single species with a rhombic g-tensor or two electronically different species, was provided by Q-band (35 GHz) EPR studies at 2 K, see Figure 5. For comparison, spectra of native protein are also shown. Note that these are dispersion mode spectra taken under "rapid-passage" conditions and thus have an "absorption" line shape.[22] At Q-band, a doublet with splitting of $A(Tl) \approx 13$ mT is clearly apparent. The microwave frequency (magnetic field) independence of this splitting confirms that it is due to hyperfine coupling to a single $^{203,205}Tl$. At 2 K, there is a relatively larger contribution to the overall EPR envelope from native cluster than in higher temperature spectra. The exact amount of this contribution is difficult to determine, since the two signals are differentially sensitive to instrumental parameters.

The X- and Q-band EPR spectra taken together clearly demonstrate that a single Tl^+ binds to the $[Fe_3S_4]^+$ cluster in *P. furiosus* Fd. The magnitude of $^{203,205}Tl$ hyperfine coupling, ~13 mT, is as large as that observed for several of the organic and inorganic small molecule systems described above. This indicates a strong Tl^+–cluster interaction and is consistent with the formation of cubane $[TlFe_3S_4]^{2+}$ cluster. Furthermore, the variable-temperature studies show that the broad, fast-relaxing "g-distribution" signal seen in the native cluster is replaced by a slower-relaxing, conventional $S = {}^1/_2$ signal. This clearly suggests that Tl^+ binding to the tri-μ_2-sulfido face "locks in" a specific cluster conformation or microenvironment. That is, Tl^+ binding leads to a unique set of D_i and J_{ij} parameters for the cluster Fe^{3+} ions.

The studies of Butt *et al.*[15] on Tl^+ binding to the $[Fe_3S_4]^+$ cluster of *D. africanus* Fd III can be reinterpreted in light of the results obtained here for *P. furiosus* Fd. Their communication only briefly described the X-band EPR spectra (without figures); however, it seems likely that the reported features at $g = 2.042$ and 1.954 correspond to the positive maximum of the low-field component and the negative minimum of the high-field component, respectively, of a $^{203,205}Tl$-split doublet. This g-value difference converts to ~15 mT for typical X-band microwave frequencies of 9.0–9.5 GHz, compared to ~17 mT for the same measurement with the $^{203,205}Tl$-split doublet of the $[TlFe_3S_4]^{2+}$ cluster in *P. furiosus Fd.* The remaining feature reported at $g = 1.993$ is likely due to the superposition of resonances from $[Fe_3S_4]^+$ and $[TlFe_3S_4]^{2+}$ clusters. On the basis of the magnitude of the $^{203,205}Tl$ hyperfine coupling constants, it thus appears that a single Tl^+ binds in a similar manner to the $[Fe_3S_4]^+$ cluster in both of these Fds.

The Tl^+-bound cluster of oxidized *P. furiosus* Fd was also investigated by Q-band ENDOR. The large $^{203,205}Tl$ hyperfine coupling observed by EPR (13.3 mT = 370 MHz at $g \approx 2.0$), combined with its Larmor frequency (at 1.240 T, $\nu(^{203}Tl) = 30.67$ MHz and $\nu(^{205}Tl) = 30.96$ MHz; these frequencies are too close to be resolved), leads to calculated ENDOR frequencies (using eq 1) of 217 and 153 MHz for ν_+ and ν_-, respectively, above the limit of our current rf instrumentation. However, a weak but

distinct ENDOR signal was observed at ~30 MHz that was absent in the spectrum of native protein (data not shown). As the magnetic field of observation ($\mathbf{B}_0$) was changed, this signal shifted correspondingly as expected for the Larmor frequency of ^{203,205}Tl (e.g., from 30 MHz at $\mathbf{B}_0$ = 1.2355 T to 33 MHz at $\mathbf{B}_0$ = 1.3525 T). It can thus be assigned to unincorporated Tl^+. The observation of such a signal is not surprising, given the large nuclear moment of ^{203,205}Tl, but is notable in that it represents the first observation of ^{203,205}Tl ENDOR in a biological system. This ^{203,205}ENDOR signal was observed across the EPR envelope of the native "*g*-distribution" cluster, indicating that it is associated with the majority of the cluster, which does not actually have an incorporated Tl^+. No signals due to ^{203,205}Tl with resolved hyperfine splitting were observed because of instrumental limitations.

The interaction of Cs^+ with the $[Fe_3S_4]^+$ cluster in *P. furiosus* Fd gave quite different EPR/ENDOR results. Few EPR/ENDOR studies have been performed involving this nucleus (^{133}Cs, $I = {}^7/_2$, $g_N = 0.7378$, $Q = 0.003 \times 10^{-24}$ cm², 100% natural abundance). Examples include γ-irradiated CsH_2AsO_4[38] and the sodide complex Cs^+(HMHCY)Na^-, where HMHCY is the macrocyclic amine ligand hexamethylhexacyclen.[39] In this latter complex, three types of hyperfine interaction with ^{133}Cs were observed. The axial EPR spectrum of this sodide complex exhibits an octet due to strong coupling to a single Cs^+ nucleus with $A_\perp^{Cs}$ = 260 MHz and $A_\parallel^{Cs}$ = 300 MHz. The large isotropic component of this coupling (270 MHz) is due to significant unpaired electron density at Cs^+.[39] A ^{133}Cs ENDOR doublet signal was observed centered at 2.1 MHz (ν_{Cs} at 0.373 T), arising from coupling to a more distant Cs^+ nucleus. This ^{133}Cs ENDOR signal was successfully simulated using the following parameters $A^{Cs} = 0.31$ MHz and $P^{Cs} = 5.3$ MHz.[39] A subsequent pulsed-EPR (ESEEM) study showed a third type of weakly coupled Cs^+ with $A^{Cs} = 0.01$ MHz (in addition to a site with $A^{Cs} = 0.34$ MHz).[40] However, computer simulations of the ESEEM data suggested that quadrupole coupling for the $A^{Cs} = 0.34$ MHz site equaled zero. Additionally, in a recent study of Mn^{2+}- and VO^{2+}-substituted pyruvate kinase, ^{133}Cs ESEEM was detected.[41] In this case, the only feature due to ^{133}Cs observed in the transformed data was a narrow signal at ν_{Cs}.

The EPR spectra of the $[Fe_3S_4]^+$ cluster in *P. furiosus* Fd in the presence and absence of excess Cs^+ (up to 1000-fold excess) are virtually superimposable (data not shown). There is therefore no extensive spin delocalization onto Cs^+ from the cluster, nor does Cs^+ "lock in" a single electronic microenvironment, in contrast to Tl^+. Thus it seems clear that Cs^+ is not incorporated into the $[Fe_3S_4]^+$ cluster. However, ENDOR does show interaction between a Cs^+ ion and the cluster. Figure 6 presents the low-frequency Q-band ENDOR spectra of oxidized 3Fe *P. furiosus* Fd as native protein and in the presence of a 30-fold excess of Cs^+. The native protein exhibits only a featureless base line over this low-frequency rf range, despite the fact that it does give rise to a strong ^{1}H ENDOR pattern as well as a weaker signal at ~13 MHz that is assigned to ^{13}C in natural abundance (data not shown). Similar natural-abundance ^{13}C signals from the protein matrix have been reported for many Fe–S proteins.[42] In contrast, the Cs^+-containing sample exhibits a broad ^{133}Cs ENDOR signal. The signal begins at $\nu \leq 2$ MHz and extends to $\nu \geq 12$ MHz, with resolved features near ν_{Cs} (6.9 MHz at 1.236 T). As is often the case, the signal shifts ~0.3 MHz in the rf sweep direction; forward and reverse rf scans average to exactly ν_{Cs}. Interestingly, in order

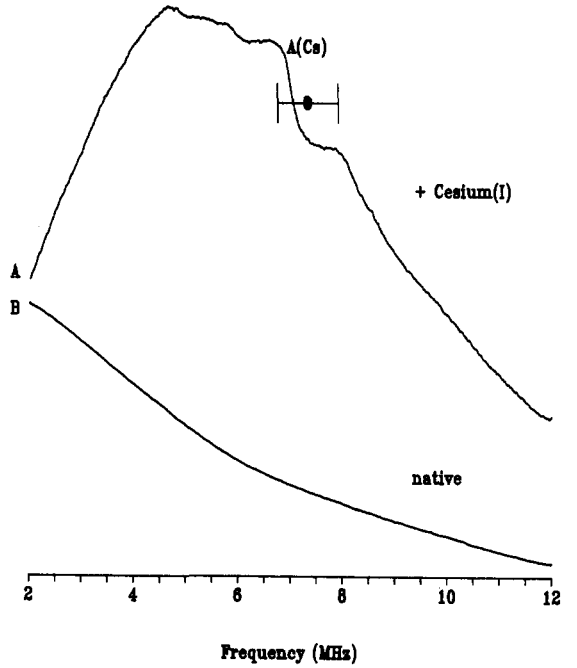

Figure 6. Q-band ENDOR spectra of the oxidized $[Fe_3S_4]^+$ cluster in *P. furiosus* Fd in the presence (A) and absence (B) of a 30-fold molar excess of CsCl. Samples are as described in Figure 4. Experimental conditions: temperature, 2 K; time constant, 32 ms; rf scan rate, 1 MHz/s; rf power, 40 W; 100-kHz magnetic field modulation amplitude, 0.07 mT; microwave frequency, 35.07 GHz (native) and 35.10 GHz (Cs^+-treated); microwave power, 2 mW (native) and 1.3 mW (Cs^+-treated); magnetic field, 1.2360 T; number of scans, 100 (native) and 500 (Cs^+-treated). No base-line correction was used. The relative intensities of the native and Cs^+-treated samples are arbitrary; no attempt at normalization was made. An assignment of two spectral features to a ^{133}Cs hyperfine-split doublet (A(Cs) ~ 1 MHz) is indicated. The center of this doublet (●) would correspond to the Larmor frequency of ^{133}Cs (ν_{Cs} = 6.9 MHz), except that the spectrum is shifted by ~0.3 MHz in the scan direction.

to observe this ^{133}Cs ENDOR signal clearly, higher microwave power was required than that optimal for observing ^{1}H ENDOR on the same sample (1.3 versus 0.3 mW, respectively). Qualitatively, this may be due to the faster relaxation time of this high-spin nucleus. This result represents the first observation of ^{133}Cs ENDOR in a biological system, and, combined with the recent ^{133}Cs ESEEM,[41] it suggests that this readily available nucleus could become more widely used as a probe of monocation binding in paramagnetic biomolecules, particularly those involving physiological Na^+ or K^+.

The spectra in Figure 6 were recorded with the magnetic field set near the dispersion mode EPR signal maximum; the only well-defined *g*-value. Similar but weaker signals were obtained at higher field positions. In metalloproteins with well-defined *g*-values, the field dependence of ENDOR signals from many types of nuclei (^{1}H, ^{2}H, ^{13}C, etc.) has been used to determine the full hyperfine tensor. Unfortunately, this is not possible for most $[Fe_3S_4]^+$ cluster because of the distribution of *g*-values.[32]

Nevertheless, a qualitative analysis of the ^{133}Cs ENDOR pattern can be obtained by analogy with earlier work on the ^{95}Mo ($I = {}^5/_2$) ENDOR signal seen in the MoFe protein of nitrogenase from *Klebsiella pneumoniae*.[43] In that system, a broad feature was observed, along with a superimposed sharp feature near ν_{Mo} that was assigned to the ν_- peak of the $m_I = \pm{}^1/_2$ nuclear transition. By analogy with that analysis, we can assign the two most distinct features centered about ν_{Cs} to transitions between $m_I = \pm{}^1/_2$ states. The separation between these features corresponds to A^{Cs}

(38) Kahol, P. K.; Dalal, N. S. *Solid State Commun.* **1988**, *65*, 823–827.
(39) Ellaboudy, A. S.; Bender, C. J.; Kim, J.; Shin, D.-H.; Kuchenmeister, M. E.; Babcock, G. T.; Dye, J. L. *J. Am. Chem. Soc.* **1991**, *113*, 2347–2352.
(40) McCracken, J.; Shin, D.-H.; Dye, J. L. *Appl. Magn. Reson.* **1992**, *3*, 305–316.
(41) Tipton, P. A.; McCracken, J.; Cornelius, J. B.; Peisach, J. *Biochemistry* **1989**, *28*, 5720–5728.
(42) Houseman, A. L. P.; Oh, B.-H.; Kennedy, M. C.; Fan, C.; Werst, M. M.; Beinert, H.; Markley, J. L.; Hoffman, B. M. *Biochemistry* **1992**, *31*, 2073–2080.
(43) True, A. E.; McLean, P.; Nelson, M. J.; Orme-Johnson, W. H.; Hoffman, B. M. *J. Am. Chem. Soc.* **1990**, *112*, 651–657.

$\approx$ 1.2 MHz. The overall breadth of the ENDOR pattern ($\Delta\nu \geq$ 10 MHz; to first-order $18P$) can then be used to provide an estimate of $P \approx 0.5$ MHz. In an effort at further quantitation, the exact solution of the full nuclear spin Hamiltonian was used to generate primary ENDOR transition frequencies and probabilities at the well-defined g-value (for this purpose, an isotropic $g = 2.03$ was used). The overall breadth of the ^{133}Cs ENDOR pattern could be qualitatively reproduced using $P_z = 0.75$ MHz (for simplicity, no rhombic component was used, i.e., $\eta = 0$); values significantly removed from 0.75 did not successfully match the breadth of the pattern. The value chosen for A^{Cs} (an isotropic A^{Cs} was used) had a lesser effect (within the range $0.5 \leq A^{Cs} \leq 1.5$ MHz), regardless of the choice of P_z. However, $0.5 \leq A^{Cs} \leq 1.5$ MHz gave the best agreement with the features near ν_{Cs}. Combining these two methods of analysis gives $P_z = 0.7 \pm 0.3$ MHz and $A^{Cs} = 1.2 \pm 0.3$ MHz as reasonable estimates. Thus, the observed ^{133}Cs ENDOR pattern can be understood by assuming that is is due to a single Cs^+ ion in a well-defined binding site. However, the low resolution of this ^{133}Cs ($I = {}^7/_2$) signal dictates that one cannot rule out the possibility of there being a distribution of hyperfine and/or quadrupole coupling constants arising from slightly different Cs^+ binding environments.

Some conclusions can be drawn as to the Cs^+ environment based on the estimated magnetic parameters. The small A^{Cs} value does not *necessarily* indicate a negligible interaction with the $[Fe_3S_4]^+$ cluster because we do not known the spin distribution within the cluster. However, we can compare the Cs^+ and Tl^+ hyperfine couplings. As calculated by Morton and Preson,[44] an unpaired electron in a thallium 6s orbital would have an isotropic hyperfine coupling of 183 800 MHz, while for atomic cesium, A_{iso} is only 2467 MHz. If we were to assume that Cs^+ and Tl^+ bind to the same cluster site, then the value of $A^{Tl} \approx 370$ MHz measured for the Tl^+-incorporated cluster would translate to $A^{Cs} \approx 5$ MHz for identical bonding. Conversely, a Tl^+ ion bound similarly to the Cs^+ observed by ENDOR might be expected to have $A^{Tl} \approx$ 40–80 MHz, and no such signals were detected by ENDOR. Thus, the Cs^+ interaction with the cluster not surprisingly appears to be much less covalent than that for Tl^+. The ^{133}Cs quadrupole coupling constant (P_z) is comparable to those shown[21] by coordinated histidine ^{14}N, although the ^{133}Cs quadrupole moment (Q) is about 6-fold lower.[33] This indicates a substantial asymmetry in the coordination environment of Cs^+. A specific interaction between Cs^+ and one or more protein residues (e.g., carboxylates) near the cluster satisfies the criteria of low hyperfine coupling and large electronic distortion.

Both RR and MCD were also used to probe the interaction of Tl^+ and Cs^+ with the $[Fe_3S_4]^+$ form of the cluster. The presence of up to 1000-fold excess Tl^+ or Cs^+ did not significantly perturb the temperature-dependent MCD spectrum of the $[Fe_3S_4]^+$ cluster in *P. furiosus* Fd (data not shown).[12] This is not surprising for Cs^+, where the interaction is likely to be largely ionic, and the EPR spectrum is unperturbed. In the case of Tl^+, the parallel EPR data indicated that only $\sim$20% of the clusters were present as well-defined $[TlFe_3S_4]^{2+}$ clusters. It therefore seems likely that the MCD spectrum is completely dominated by the $[Fe_3S_4]^+$ cluster and that the minor component (i.e., $[TlFe_3S_4]^{2+}$) is not observed.

Both excess Cs^+ and excess Tl^+ produced the same small but significant and reversible changes in the RR spectrum of the $[Fe_3S_4]^+$ cluster in *P. furiosus* Fd, see Figure 7. The changes were complete with 30-fold and 1000-fold excesses of Cs^+ and Tl^+, respectively. The vibrational modes of the $Fe_3S_4{}^bS_3{}^t$ unit have been assigned under effective C_{3v} symmetry based on normal mode calculations and $^{34}S^b$ isotope shifts.[28] The bands at 386 and 368 cm^{-1} are assigned primarily to Fe–S^t stretching ($\leq$2-cm^{-1} $^{34}S^b$-downshifts), whereas the bands at 405 (sh), 397, 347, 289, and 263 cm^{-1} are assigned primarily to Fe–S^b stretching

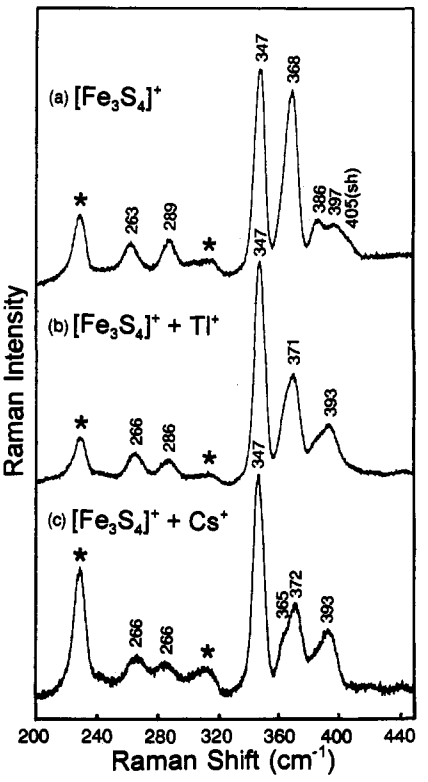

Figure 7. Low-temperature resonance Raman spectra of the oxidized $[Fe_3S_4]^+$ cluster in *P. furiosus* Fd in the presence of excess Cs^+ and Tl^+. (a) As prepared, (b) with 1000-fold molar excess of $Tl(OOCCH_3)$; and (c) with 30-fold molar excess of CsCl. The sample concentrations were 1.1, 1.2, and 0.85 mM, for spectra a, b, and c, respectively, and the buffer was 50 mM Tris-HCl, pH 7.8. The spectra were obtained at 17 K using 488.0-nm laser excitation and are the sum of 16 scans. Each scan involved photon counting for 1 s at 0.2-cm^{-1} increments with 6-cm^{-1} spectral resolution. Bands marked with an asterisk are lattice modes of the frozen buffer solution.

($\geq$4-cm^{-1} $^{34}S^b$-downshifts). The shifts seen in both Fe–S^b and Fe–S^t modes on the addition of excess Tl^+ or Cs^+ are significant, but the frequencies and pattern of bands are still characteristic of a $[Fe_3S_4]^+$ cluster. Based on the RR studies of Tl^+ binding to the reduced $[Fe_3S_4]^0$ cluster, much more dramatic differences in the RR spectra would be expected to accompany actual incorporation of the metal monocation to form cubane $[TlFe_3S_4]^{2+}$ or $[CsFe_3S_4]^{2+}$ clusters. Rather small changes in one or more of the cysteine Fe–S_γ–C_β–C_α dihedral angles could easily account for the observed effects. Again, it seems likely that the RR spectrum of the Tl^+-treated sample is completely dominated by the $[Fe_3S_4]^+$ cluster and that the minor component (i.e., $[TlFe_3S_4]^{2+}$) is not observable by RR due to its low concentration and/or weaker resonance enhancement. The changes in the RR spectra of the $[Fe_3S_4]^+$ cluster in the presence of excess Tl^+ or Cs^+ both are therefore attributed to protein conformational changes induced by binding one (or more) of these large ions to residue(s) in the vicinity of the majority, native cluster form. It seems likely that the ^{133}Cs ENDOR signal is associated with a single protein-bound ion. The asparate residue that may be directly involved in coordinating the removable Fe atom is an obvious candidate for this ion-binding site, because parallel studies with excess Cs^+ (and Tl^+) did not result in any significant perturbation in the RR spectrum of the $[Fe_4S_4]^{2+}$ center in *P. furiosus* Fd.

Conclusions

Removal of an iron atom from a 4Fe Fd exposes a tri-μ_2-sulfido face to which a different metal ion can then bind. This exogenous metal binding is generally enhanced by the presence

(44) Morton, J. R.; Preston, K. F. *J. Magn. Reson.* **1978**, *30*, 577–582.

of reducing agent (chemical or electrochemical) that yields formally an electron-rich $[Fe_3S_4]^-$ cluster. This leads to the formation of $[MFe_3S_4]^{2+/+}$ cluster via interaction with divalent (Zn^{2+}, Co^{2+}, Ni^{2+}, Mn^{2+}, Cd^{2+}) or trivalent (Ga^{3+}) metal ions.[9-11] These reduced clusters can, in some cases, be oxidized by one electron with retention of the exogenous metal ion to give $[MFe_3S_4]^{2+}$ clusters, e.g., M = Co and Zn.[9-11] Here we have investigated the binding of large, polarizable monocations (M^+ = Cs^+, Tl^+) to the 3Fe cluster of *P. furiosus* Fd in the absence of any chemical or electrochemical reducing agent, to determine if such redox-unassisted metal binding can occur. The specific M^+ ions were selected for their large size and polarizability. However, the two represent extremes of ionic versus covalent interactions with sulfide: extensive covalent interactions with Tl^+ and minimal covalent interactions with Cs^+. This chemical difference is dramatically manifested in their interaction with the $[Fe_3S_4]^0$, cluster in *P. furiosus* Fd.

MCD studies of monocation binding to the reduced, $S = 2$ $[Fe_3S_4]^0$ cluster of *P. furiosus* Fd show that the cluster remains intact and that its electronic structure is strongly perturbed by Tl^+. In particular, the S → Fe charge-transfer bands shift to lower energy as a result of additional electron density on S provided by the electron-rich ($6s^25d^{10}$) Tl^+. The incorporation of Tl^+ to form $[TlFe_3S_4]^+$ by metal binding to the tri-μ_2-sulfido face of the $[Fe_3S_4]^0$ cluster is clearly indicated by dramatic changes in the cluster vibrational modes, as evidence by RR studies. No such effects are seen with ($6s^05d^0$) Cs^+, indicating that Cs^+ is not incorporated.

Tl^+ and Cs^+ binding to the oxidized $S = {}^1/_2$ $[Fe_3S_4]^+$ cluster were also investigated. The affinity for Tl^+ of the oxidized cluster is much lower than that for the reduced $[Fe_3S_4]^0$ cluster. However, excess Tl^+ does convert 10–20% of the oxidized clusters to a species with an EPR spectrum no longer having the *g*-distribution appearance, indicating a single cluster conformation. The observation by EPR of a large, isotropic $^{203,205}Tl$ hyperfine coupling ($A^{Tl} \approx 370$ MHz, 13 mT) at two microwave frequencies (X- and Q-band) conclusively showed that this species is due to $[TlFe_3S_4]^{2+}$ formed by incorporation of a Tl^+ ion into to the $[Fe_3S_4]^+$ cluster. The magnitude of this $^{203,205}Tl$ hyperfine coupling is comparable to that found in thallium-containing organic and inorganic radical ion pairs.[34,35] Large ^{133}Cs hyperfine couplings have been observed in a Cs^+-containing radical ion pair.[39] However, no such coupling was observed for the $[Fe_3S_4]^+$ cluster in the presence of excess Cs^+, nor did the EPR spectrum differ from that of the native cluster. This indicates that Cs^+ also is not incorporated into the oxidized cluster. However, RR studies indicate that excess Cs^+ (and Tl^+) do perturb the native $[Fe_3S_4]^+$ cluster structure, presumably via binding to nearby protein residues. ^{133}Cs ENDOR provides evidence that a Cs^+ ion is bound near the cluster in a well-defined site. A likely site is the aspartate residue that presumably coordinates the removable Fe ion in the 4Fe form of *P. furiosus* Fd. In support of this, the $[Fe_4S_4]^{+,2+}$ cluster is unaffected by these monocations. This work will be extended to investigations of the binding of low-valent transition metals (e.g., Ni(I) or Ni(0)), that may have relevance to catalytic Fe–S proteins.

Acknowledgment. This work was supported by grants from the NSF (DMB-8907559 to B.M.H., a Research Opportunity Award to J. T., Research Training Group Award DIR-9014281 to the Center for Metalloenzyme Studies, and instrumentation grant DIR-9102055 to M.K.J.) and the NIH (GM-45597 to M.W.W.A. and M.K.J.).